

GaFET: Learning Geometry-aware Facial Expression Translation from In-The-Wild Images

Tianxiang Ma^{1,2*}, Bingchuan Li^{3*}, Qian He³, Jing Dong^{2†}, Tieniu Tan^{2,4},

¹School of Artificial Intelligence, UCAS ²CRIPAC & NLPR, CASIA

³ByteDance Ltd, Beijing, China ⁴Nanjing University

tianxiang.ma@cripac.ia.ac.cn, {libingchuan, heqian}@bytedance.com, {jdong, tnt}@nlpr.ia.ac.cn

Abstract

While current face animation methods can manipulate expressions individually, they suffer from several limitations. The expressions manipulated by some motion-based facial reenactment models are crude. Other ideas modeled with facial action units cannot generalize to arbitrary expressions not covered by annotations. In this paper, we introduce a novel Geometry-aware Facial Expression Translation (GaFET) framework, which is based on parametric 3D facial representations and can stably decouple expression. Among them, a Multi-level Feature Aligned Transformer is proposed to complement non-geometric facial detail features while addressing the alignment challenge of spatial features. Further, we design a De-expression model based on StyleGAN, in order to reduce the learning difficulty of GaFET in unpaired “in-the-wild” images. Extensive qualitative and quantitative experiments demonstrate that we achieve higher-quality and more accurate facial expression transfer results compared to state-of-the-art methods, and demonstrate applicability of various poses and complex textures. Besides, videos or annotated training data are omitted, making our method easier to use and generalize.

1. Introduction

Photo-realistic face expression generation and manipulation have rich practical application scenarios, such as portrait photo beautification, face emotion control, and movie industry production. However, expression as a face attribute is highly bound with face shape, texture, lighting and other factors, which makes it difficult to transfer and manipulate effectively. These factors bring a lot of challenges to the expression translation task.

Early GAN-based expression synthesis and translation

methods [44, 39, 31, 26] suffer several limitations, among which the most painful problem is the low quality of synthesized images. They are usually generated at 128 resolution or below, which naturally loses a lot of expression detail. Another idea [4, 32] relies on specific face expression category labels for cross-domain image-to-image translation. The most common are the 8 basic expression categories such as happy, sad, surprised, etc. But these completely limit the diversity of facial expressions. More novel approaches [26, 20] utilize action units (AUs), which describe the anatomical facial movements that define human expressions in a continuous manifold. It is equivalent to splitting the expression annotations of the whole face image into multiple sets of local expression annotations. Although AUs are more fine-grained than image categories, it is still difficult to accurately describe arbitrary face geometries at such a high level of abstraction.

Another expression-related face reenactment techniques [30, 9, 2, 38, 5, 6] have been widely developed. They usually require a large amount of video data for self-supervised training, and use the reference head motion video to drive the target face during the inference process. However, since large motions and deformations (e.g. pose changes) are the focus of this task, these methods usually ignore fine-grained expression synthesis. Blurring, deformation, and distortion are common in face reenactment methods. In addition, some reenactment methods such as FOMM [30] and DaGAN [11] cannot decouple expressions automatically. Therefore, when comparing and evaluating these methods, the reference images of pose and shape pairings are artificially selected to eliminate their disadvantages for expression transfer as much as possible.

Aiming at the difficulties of current expression manipulation, we propose a novel geometry-aware facial expression translation (GaFET) method to improve it. First, we adopt 3D face geometry to represent expressions, in order to avoid class annotations limiting the generative diversity. We introduce state-of-the-art 3D face parametric model EMOCA [3], which has the most accurate and stable

*These authors contributed equally.

†Corresponding author.

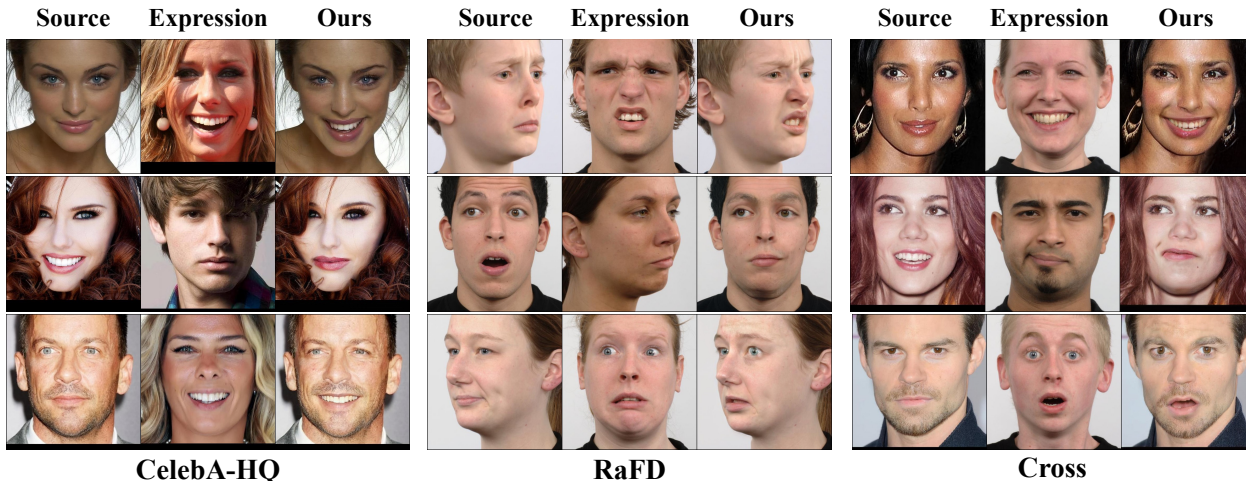


Figure 1. High-quality face expression transfer results obtained by our method on the 512 resolution CelebA-HQ and RaFD datasets. The “Cross” represents the cross expression transfer on that two datasets.

expression representation so far. Specifically, we use the EMOCA encoder to extract expression features from the reference face with other expression-independent features from the source face, and then combine them, and differentially render a 3D geometric image. Therefore, it has the pose and shape of the source face and maintains the expression characteristics of the reference face.

Moreover, we found that 3D parametric geometry alone cannot fully represent fine expression information. For this reason, we propose a Multi-level Feature Aligned Transformer (MFAT) network that helps to extract texture details from expression image to complement the lack of geometric features, like teeth details. Since the source and expression faces may have different poses and shapes, spatially aligning detailed features and geometric features becomes a challenge. Our proposed MFAT has a global receptive field and can efficiently align local expression features through self-attention and cross-attention mechanisms. We add the multi-level features learned from MFAT to the spatial features learned from 3D geometry in the form of residuals to complete the expression details.

Considering the high acquisition cost of video or labeled images, our model is built on unlabeled and unpaired “in-the-wild” images, so it is easier to apply more high-quality images for learning. Particularly, we design an emotion removal method based on StyleGAN’s latent space editing and incubate a De-expression model to reduce the learning difficulty of unpaired images. It helps GaFET compute the reconstruction loss using the pseudo-paired data constructed by the De-expression model. GaFET is trained in a generative adversarial manner, where we carefully design the generator structure, including proposing a spatial and global modulation module and integrating a multi-level fea-

ture deformation module [42], while adding an additional local discriminator for quality of detail. Experiments verify the excellent generalization performance of our method. The main contributions can be summarized as follows:

- We propose a novel geometry-aware facial expression translation framework that achieves high-quality expression transfer.
- We further propose a Multi-level Feature Aligned Transformer module to extract detailed features and spatially align them with geometric features.
- The De-expression model is designed based on StyleGAN, which reduces the difficulty of training on unlabeled and unpaired “in-the-wild” images.
- Compared with SOTA facial expression manipulation methods, we have clear advantages in performance and ease of use.

2. Related Work

2.1. Facial Expression Synthesis and Transfer

Expression synthesis and transfer is a long-studied task. Early approaches [33, 34] relied on professional RGB-D camera to capture the face geometry and target the design of character-specific expression transfer. Later, Some methods [44, 39, 4, 31] started to explore the optimization of network structure to enhance expression transfer. Pumarola et al. [26] proposed to use face action units as conditional input for expression features and added an alpha channel output. Yang and Lim [41] used pre-trained StyleGAN to do unconstrained expression transfer. Fan et al. [7] started to consider image to video face expression transfer and extended

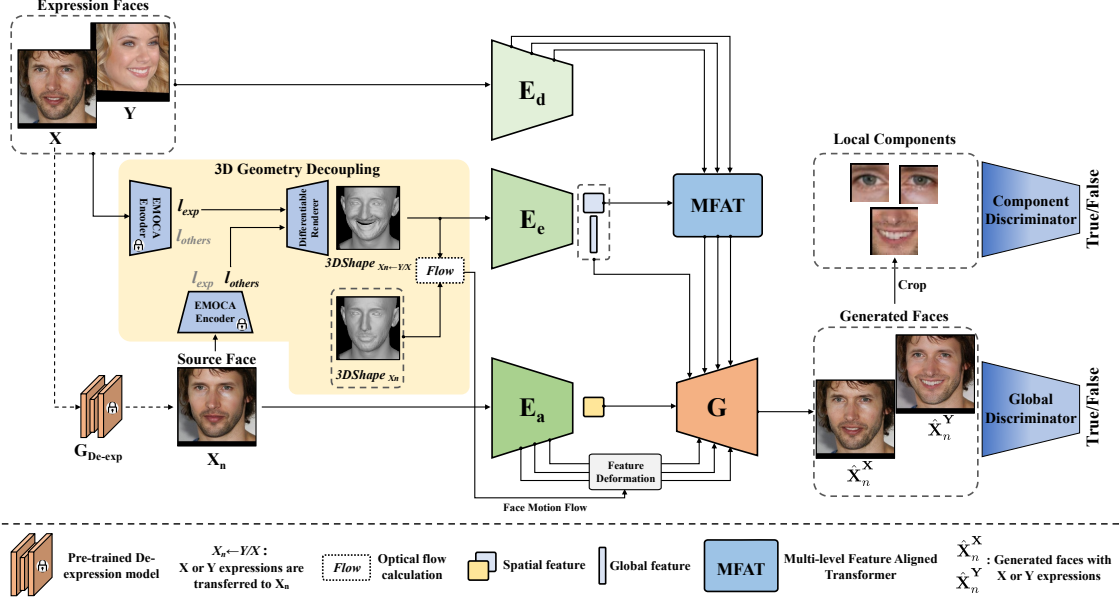


Figure 2. The overall framework of our GaFET. The 3D geometry decoupling module provides a geometry-aware expression representation, where expression-related features are derived from reference expression faces, and other expression-independent attributes are derived from source faces. The three encoders E_d , E_e , and E_a extract features from the expression reference face, 3D shape, and source face, respectively. The MFAT spatially aligns and fuses expression-related features. The pre-trained De-expression model offers pseudo-paired data to help model training. The *Flow* calculates facial geometric motion to deform source face features.

it with some interesting applications. Wang et al. [37] explicitly decoupled face deformations and appearance details by constructing two parallel networks. Tang et al. [32] proposed an expression conditional GAN model and use the binarized expression category vectors to guide model generation and training. Wu et al. [40] proposed a progressive network with special attention to improve the expression transfer effect. Ling et al. [20] also use face action units as conditional input, but they use the variations of AUs to guide expression synthesis. Jourabloo et al. [14] implemented 3D reconstruction of facial expressions based on face data captured by VR devices.

2.2. Face Reenactment and Talking Head

Face reenactment and talking head generation are the tasks very relevant to expression synthesis, which aims to transfer the head pose and movement that incorporate expressions. Earlier, Nirkin et al. [24] proposed a recurrent neural network-based face reenactment and face swapping method. Siarohin et al. [30] first proposed a first-order motion model that is capable of unsupervised learning of face animation. Tripathy et al. [35] proposed an interpolable face animator, which is driven by head pose angles and face action units. Gu et al. [8] used landmark as the driving input for talking face. Ha et al. [9] proposed a series of modules to achieve high-quality face reenactment. Burkov et al. [2] designed a neural head reenactment model that

drives the head through a latent pose representation. Zhang et al. [46] used face landmark as the vehicle to train a unified landmark converter and a geometry-aware generator. Wang et al. [38] proposed a neural talking-head generation method based on decoupled keypoint representation. Recently, Hong et al. [11] introduced a self-supervised face-depth learning method to assist in talking-head generation. Yin et al. [45] used a pre-trained StyleGAN model and learned spatial transformation in the latent space to achieve talking face generation. Doukas et al. [5] introduced high-resolution face reenactment method based on 3DMM parametric model and Yang et al. [42] further improved it into a real-time algorithm. Yang et al. [43] proposed a 3d-aware face editing method, which can drive facial expressions. Lyu et al. [21] introduced a text-driven face manipulation approach, which is suitable for simple expression editing. Hsu et al. [12] proposed a dual-generator structure to learn face reenactment in large poses. Drobyshev et al. [6] designed specific architecture and training procedure that encourages disentanglement between motion and appearance.

3. Approach

In this section, we will introduce the geometry-aware facial expression translation framework in detail. Since there is no paired or annotated facial expression data, we designed a semi-supervised approach to help model training by introducing a portion of pseudo-paired data. Consider a

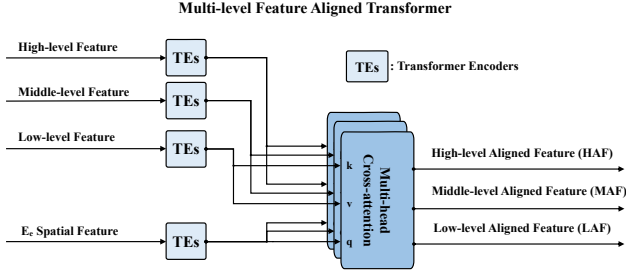


Figure 3. Detailed structure of the MFAT module.

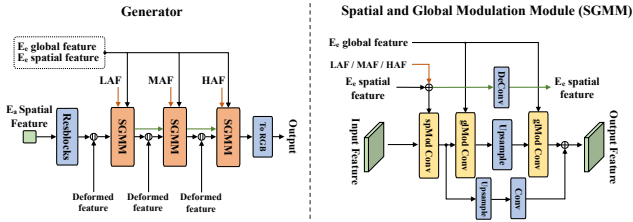


Figure 4. Detailed structure of the facial expression Generator.

source face X and a reference expression face Y , and expect to generate a new face that maintains the identity of X and has the expression of Y , denoted by \hat{X}^Y . To construct pseudo-paired data, we introduce a pre-trained De-expression model $G_{\text{De-exp}}$, which removes as much expression as possible from a source face X to generate neutral face X_n . Therefore, we can use X_n and X as the source image and reference image respectively, generate \hat{X}_n^X , and perform reconstruction constraints with X . Meanwhile, we also use the unpaired Y as a reference expression to generate \hat{X}_n^Y , and focus more on the identity-independent facial geometry loss. The framework optimizes these two input modes in parallel for sufficient learning. The overall framework is shown in the Figure 2. In the following parts, the model details are presented.

3.1. 3D Geometry Decoupling

Since facial expression features and the facial shape are highly correlated, it is desirable to effectively separate the two attributes. We introduce an emotion-driven face capture method EMOCA [3], which can well decouple the expression, shape, and pose attributes of the face. We utilize EMOCA encoder to extract expression-independent feature coefficients (l_{others}) such as global pose and shape from the source face, and expression and jaw feature coefficients (l_{exp}) from the reference expression face. These coefficients are combined and the 3D geometry is decoded and reconstructed based on FLAME [19]. Then we utilize the expression encoder E_e to learn spatial and global features from input 3D geometry. Besides, we also render the motion flow between the source 3D vertices and the 3D vertices

of combination coefficients to facilitate feature warping operations in the generator. The modeling process for this part is shown on the left side of the figure 2.

3.2. Multi-level Feature Aligned Transformer

Since the 3D geometry lacks the detailed information of the face texture, like teeth, it cannot fully represent the expression. The straightforward idea is to extract detailed texture features from reference expression face to complement the missing information in 3D geometry. Since the poses and shapes of the source face and the reference face are inconsistent, it is unreasonable to directly overlay the texture features with the geometric features. To address this issue, we propose a novel multi-level feature aligned transformer (MFAT) that can spatially fuse and align the two features.

The structure of the module is shown in the Figure 3. First, The encoder E_d extracts multi-level features of the reference expression face, divided into high, middle and low level features. The spatial feature learned by E_e are simultaneously obtained. Then, they are passed through a set of transformer [36] encoders separately to learn the self-attention features. This process can adaptively learn useful information of features with the help of a global multi-head self-attention mechanism, and is not affected by the spatial alignment problem. Finally, for each level, we use a multi-head cross-attention module that utilizes the spatial features extracted by E_e to query the matched features on different level, and outputs multi-level aligned features. After learning, this module can supplement the missing details of geometry.

3.3. Face Expression Generation

For a given source face, we use the appearance encoder E_a to extract spatial features as input to the expression generator backbone. The detailed structure of the proposed expression generator is shown in the Figure 4. Where SGMM is used to fuse the features extracted from different modules. Within each SGMM, the spatial and global features extracted by E_e work on different modulation networks, called spatial modulation network and global modulation network, respectively. They are similar in form to the (de)modulation modules in StyleGAN [17], and the difference lies in whether the input modulation features carry a spatial dimension. Using the global features can help to better guide the synthesis process, and its effectiveness has been demonstrated in the ablation study. We add multi-level expression-aware aligned features learned from MFAT to the E_e spatial feature as residuals. This approach can effectively combine both features to get our complete expression representations. The new spatial feature obtained at each level is passed through the deconvolutional layer to the next level of the network.

We employ a U-Net-like network structure to obtain fea-

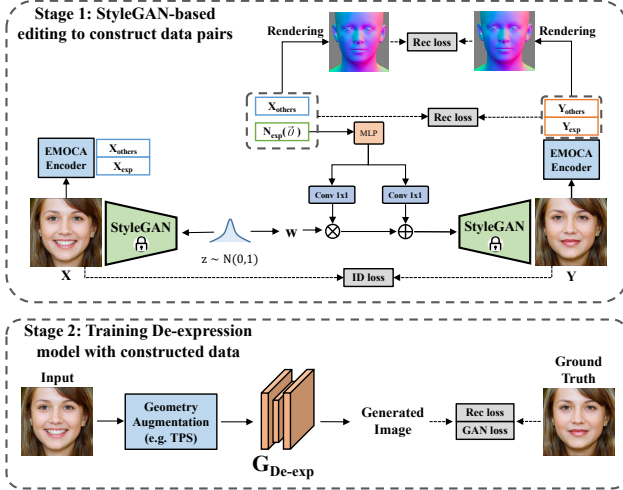


Figure 5. De-expression model training process.

tures from E_a at different scales and inject them into the generator. Meanwhile, the feature deformation [42] network is used to morph the input multi-scale E_a features by the motion flow computed from two 3D vertices. This makes it easier for the generator to perceive geometric changes in expressions. Finally, the last output layer of the generator converts the features into an RGB image, which is an expression-translated face.

3.4. Pre-trained De-expression Model

The pre-trained De-expression model is an important part of our GaFET framework to implement pseudo-paired data training. The training details of the De-expression model are shown in Figure 5. The main idea is to train a StyleGAN-based editing model to construct paired expression faces so that a De-expression model can be trained. First, we utilized a pre-trained StyleGAN [17] to train a StyleGAN-based editing model as in the upper part of Figure 5. Specifically, We use the EMOCA to extract expression coefficients and other expression-unrelated coefficients from the face generated by random sampling. The neutral expression code, i.e., zero vector, is used as the modulation parameter in editing the w code to guide the generation of the corresponding De-expression faces. The training of this editing model (MLP and Convolutional networks) is supervised by the reconstruction loss of 3DMM coefficients and rendered normal maps, while using identity loss to constraint the identity of edited face. Second, we use the trained StyleGAN-based editing model to generate 50,000 paired faces (the face and its neutral expression face), and learn a De-expression model with U2Net [27] structure as shown in the lower part of Figure 5. Further, geometric augmentations (e.g. Thin Plate Spline) are used to improve the robustness of the De-expression model during training. Please

refer to the supplementary material for the De-expression effects of this model.

3.5. Training

Discriminators. We employ two discriminators to assist in the training of our expression translation model. A global discriminator is used to discriminate the overall image, and a component discriminator is used to discriminate the eye and mouth regions of the face. Since most of the expression variations are in the mouth and eye regions, the introduction of component discriminator can help our model to better generate local expression details. During training, we extract fixed size patches of the eye and mouth regions using a pre-trained face landmark detector, and feed them into the component discriminator, which has the same structure as the global discriminator except that the number of model parameters is smaller.

Reconstruction Loss. In the training stage, we alternately feed pseudo-paired faces (X_n, X) and unpaired faces (X, Y) as model inputs. When the inputs are pseudo-paired (X_n, X), we can use the reconstruction loss to train the model with the following equation,

$$\mathcal{L}_{\text{rec}}^{\text{pseudo}} = \left\| X - \hat{X}_n^X \right\|_1 + \lambda \cdot \text{lpips}(X, \hat{X}_n^X), \quad (1)$$

where the first part is the L_1 norm reconstruction loss, and the second part is the reconstruction loss calculated using Learned Perceptual Image Patch Similarity (lpips) [47]. λ is the weight to balance loss terms.

Except for the reconstruction loss, the rest of the losses we used are the same for different input conditions. In the following, we present each loss by using (X_n, Y) as inputs.

Expression Losses. For our training task the core purpose is to transfer Y 's expression to X . We take two approaches to constrain the expression attribute of the generated face to be consistent with that of Y . First we extract the expression code of the generated face and other expression-independent codes using the same method as in the 3D geometry decoupling module. Then we replace the expression-independent codes with the Y counterpart, and use a differentiable renderer to obtain the 3D shape. We compute the reconstruction loss between that 3D shape and the reconstructed 3D shape of Y as the formula below,

$$\mathcal{L}_{\text{exp}}^{\text{shape}} = \left\| S(l_{\text{exp}}^{\hat{X}}, l_{\text{others}}^Y) - S(l_{\text{exp}}^Y, l_{\text{others}}^Y) \right\|_1, \quad (2)$$

where $S(\cdot, \cdot)$ represents the 3D shape rendering operation, $l_{\text{exp}}^{\hat{X}}$ represents the expression feature code extracted from \hat{X} , and the others are the similar. This approach achieves expression consistency constraint based on 3D reconstruction, and is superior to direct expression code constraint.

Earlier we mentioned that the 3D geometry expression representation lacks textured details. So we introduce an



Figure 6. Qualitative comparisons with face reenactment methods on expression translation.

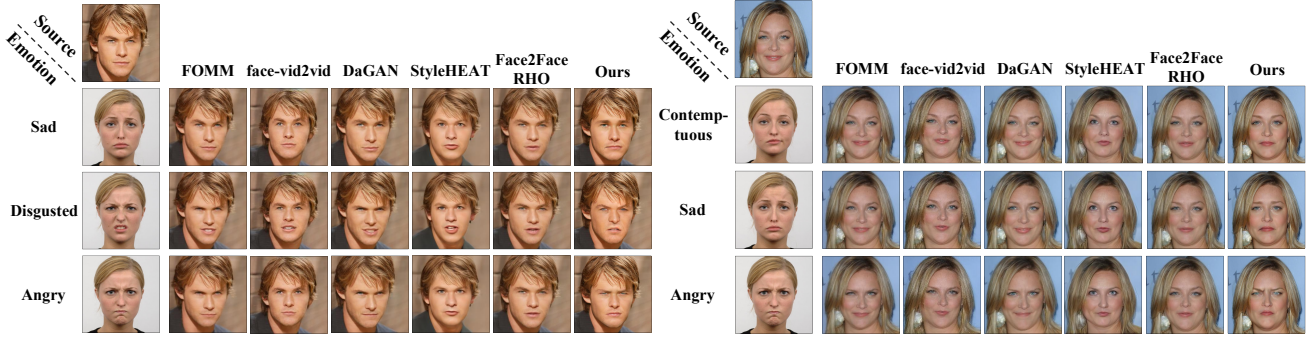


Figure 7. Qualitative comparisons with face reenactment methods on emotion manipulation.

additional facial action unit loss. We use a SOTA face action unit detection model MLCR [25], which can detect 12 action units in the face, covering cheek and eye details. We apply this model to extract action units in generated face \hat{X}_n^Y and expression face Y , respectively, and then calculate the similarity loss as the following formula,

$$\mathcal{L}_{\text{exp}}^{\text{AU}} = 1 - \text{cos_sim}(\text{AU}(\hat{X}_n^Y), \text{AU}(Y)), \quad (3)$$

where $\text{AU}(\cdot)$ represents the AU feature embedding obtained using the face action unit detector. $\text{cos_sim}(\cdot, \cdot)$ means cosine similarity.

Contextual Loss. In order to make the style and texture of the generated face consistent with the source face, we use Contextual Loss [22] to constrain the appearance features of the generated face with the following formula,

$$\mathcal{L}_{\text{cx}} = \sum_i \omega_i [-\log(\text{CX}(\phi_i(\hat{X}_n^Y), \phi_i(X_n)))] \quad (4)$$

where $\text{CX}(\cdot, \cdot)$ stands for contextual similarity, ϕ_i is the

i th layer of low-level features in the pre-trained VGG-19 network, which contain mainly the rich stylized texture of the image, and ω_i is the weight coefficients of the different layers.

Adversarial Losses. During training, we apply two sets of adversarial losses for the global discriminator and the component discriminator, and adapt an R1 regularization loss term for each discriminator. The two groups of adversarial losses are denoted as $\mathcal{L}_{\text{adv}}^{\text{global}}$ and $\mathcal{L}_{\text{adv}}^{\text{comp}}$.

In summary, we optimize the overall objective as follows,

$$\begin{aligned} \mathcal{L}_{\text{total}} = & \lambda_{\text{rec}} \mathcal{L}_{\text{rec}}^{\text{pseudo}} + \lambda_{\text{exp}}^{\text{shape}} \mathcal{L}_{\text{exp}}^{\text{shape}} + \lambda_{\text{exp}}^{\text{AU}} \mathcal{L}_{\text{exp}}^{\text{AU}} + \lambda_{\text{cx}} \mathcal{L}_{\text{cx}} \\ & + \lambda_{\text{adv}}^{\text{global}} \mathcal{L}_{\text{adv}}^{\text{global}} + \lambda_{\text{adv}}^{\text{comp}} \mathcal{L}_{\text{adv}}^{\text{comp}}. \end{aligned} \quad (5)$$

The weights of the overall objective are $\lambda_{\text{exp}}^{\text{shape}}=150$, $\lambda_{\text{exp}}^{\text{AU}}=50$, and the rest are 1.0. We set these loss weights to equalize the different loss items.

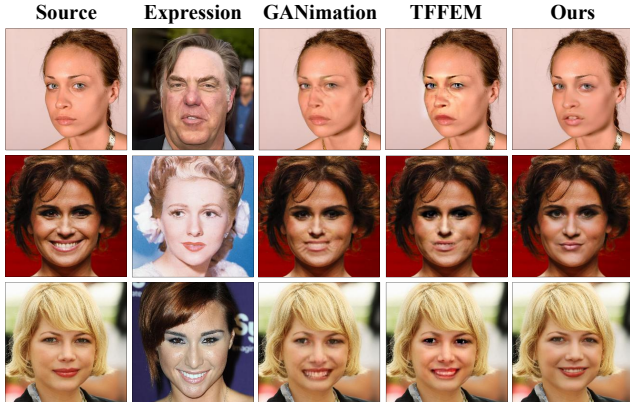


Figure 8. Qualitative comparisons with facial expression transfer methods.

	FID ↓	CSIM ↑	AED ↓	AU-H ↓
FOMM [30]	17.8	0.681	0.289	0.267
Facevid2vid [38]	42.1	0.557	0.269	0.287
DaGAN [11]	15.6	0.751	0.274	0.225
StyleHEAT [45]	35.8	0.623	0.265	0.195
Face2FaceRHO [42]	17.1	0.748	0.284	0.218
Ours	11.2	0.769	0.258	0.174

Table 1. Quantitative evaluation of our method and face reenactment methods.

4. Experiments

We conduct sufficient qualitative and quantitative experiments to compare SOTA methods, and demonstrate the superior performance of our method.

4.1. Implementation Details

Datasets. Since our method can be trained using unlabeled and unpaired “in-the-wild” data, we use the FFHQ [16] dataset and AffectNet [23] dataset as the training sets. FFHQ contains 70,000 high-quality images with rich identity attributes and style textures. AffectNet is a large-scale expression face dataset with in-the-wild images. We combined these two datasets to construct a training set of 100,000 images, and extracted face images using the same alignment as EMOCA [3]. Then we train 256 and 512 resolution version models for evaluation and comparison. In addition, to validate “in-the-wild” expression transfer effect, we use the CelebAHQ [15] and RaFD [18] datasets as the test sets, and other compared methods are similarly tested on both datasets.

Baselines. First, we compare SOTA expression translation methods GANimation [26] and TFFEM [20]. Second, considering expression translation has been gradually integrated into face reenactment and talking head, we also compare several SOTA face reenactment and talking head meth-

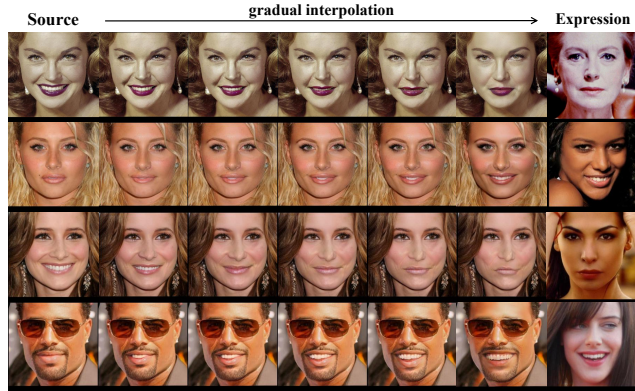


Figure 9. Progressive manipulation of expression translation.

	IS ↑	ACD ↓	ED ↓
GANimation [26]	2.71	0.396	0.315
TFFEM [20]	2.74	0.379	0.273
Ours	2.84	0.350	0.266

Table 2. Quantitative evaluation of our method with facial expression transfer methods.

ods, FOMM [30], Facevid2vid [38], DaGAN [11], StyleHEAT [45] and Face2FaceRHO [42]. Besides, to make a fair comparison with them, we choose the source and reference face with similar head pose, and focus on evaluating expression translation accuracy.

Experiment Settings. We train our model using the Adam optimizer with $\beta_1 = 0.0$ and $\beta_2 = 0.99$, and the initial learning rate is 0.002. Please refer to supplementary materials for more training details.

4.2. Quantitative and Qualitative Evaluation

We first compare with SOTA open-source available face reenactment and talking head methods, focusing on evaluating image quality and expression accuracy. We use FID [10] to measure image realism and Cosine Similarity (CSIM) of identity embeddings extracted from CurricularFace [13] to measure identity preservation after expression manipulation. Average Expression Distance (AED) [28] and Action Unit Hamming Distance (AU-H) [1] are used to count the accuracy of expression translation. As shown in Table 1, our method achieves state-of-the-art results in each measurement. Figure 6 and 7 highlight some results. Among them, since FOMM and DaGAN cannot decouple expressions automatically, we artificially separate expressions using two reference images paired with pose and shape during inference. It can be seen that the driven source image completely maintains the pose and shape, but the expression changes are still insufficient. Facevid2vid is the decoupling of 3D pose, translation and expression inside the model. However,



Figure 10. The expression translation results on the video data.

	FID ↓	CSIM ↑	AED ↓	AU-H ↓
w/o De-exp	13.4	0.712	0.301	0.208
w/o MFAT	12.2	0.730	0.286	0.183
w/o SGMM	13.1	0.739	0.264	0.179
w/o Multi-scale	11.7	0.734	0.272	0.180
w/o FD	18.4	0.701	0.340	0.215
w/o Comp. D	12.6	0.747	0.278	0.181
Ours	11.2	0.769	0.258	0.174

Table 3. Quantitative evaluation of ablation studies.

when we only modify the expression coefficients, the face undergoes an unsatisfactory drastic change. StyleHEAT generates high-quality maps, but significantly changes identity and pose. The pose of Face2FaceRHO is well maintained but the expression changes are weak. In contrast our method can transfer expressions more accurately while keeping the source face identity and appearance unchanged.

We also compare quantitatively and qualitatively with SOTA expression transfer methods. We follow the evaluation metrics of the TFFEM for quantitative evaluation. Inception Score (IS) [29] is used to evaluate the image quality. Average Content Distance (ACD) is used to measure the identity attribute gap by face recognition network. Expression Distance (ED) calculates the l_2 -distance between the AU values of the generated face and the reference face. Table 2 shows the comparison results, where our method achieves higher scores. Figure 8 shows that our method achieves better results in terms of both image quality and expressive detail.

Our approach is suitable for high-quality expression transfer, as shown in Figure 1. The source face texture preservation and reference face expression transfer are well achieved. In addition, our method not only directly translates the expression of the reference face image, but also progressively controls the degree of expression change. With the help of our geometry-aware expression representation, we are able to manipulate the face expression change

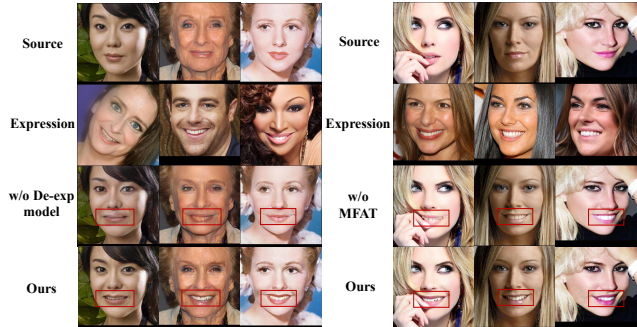


Figure 11. Qualitative comparisons of ablation studies on key modules.

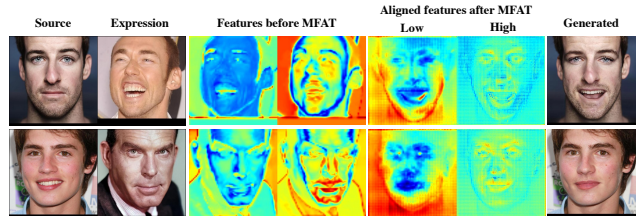


Figure 12. Feature visualization before and after the MFAT.

by interpolating the rendered face 3D vertices from the original face expression to the reference face expression. Figure 9 shows the effect of this progressive manipulation. During the gradual expression change, the generated face expressions are very natural and do not produce artifacts.

We also try to apply our method to video scenarios. As shown in Figure 10, unlike the face reenactment methods, the driving result of our method does not have any head posture movement, but only the expression motion will follow the continuous change of the driving video. Self- and Cross-identity driven results are presented.

4.3. Ablation Study

In this section, we conduct the ablation studies on several important components of our approach. The ablation studies includes: 1.remove the De-expression model; 2. remove the MFAT module 3. remove the global-modulation part of SGMM; 4. Comparison of multi-scale and single-scale attention; 5. Remove feature deformation module; 6. Remove component discriminator. Table 3 shows that there is some drop in the quality of the generated images and the accuracy of the expression transfer when removing these modules. In addition, Figure 11 intuitively shows the ablation results of two sets of innovative modules we proposed. The deformation of the mouth and the generation of teeth are the most difficult cases. When the De-expression model is removed, it can be seen from the position marked in the red box that the mouth is not opened normally. Some tooth texture details are missing or incorrect when the MFAT module is not

used. In addition, Figure 12 visualizes the input and output features of the MFAT module. It can be seen that the output features have been aligned with the source face shape, and the high-level features seem to pay attention to details.

5. Conclusion

In this paper, we propose a geometry-aware facial expression transfer method, coupled with a Multi-level Feature Aligned Transformer and a De-expression model, to achieve excellent expression transfer performance. Unlike previous expression manipulation schemes, we omit video or labeled data support, instead we can learn on more diverse “in-the-wild” data. Experimental results show that our method can generate high-resolution, high-quality, and accurate facial expression images. The limitations and bad cases are shown in the supplementary material. The future work is to steadily promote it to fit large-angle poses and exaggerated expressions.

6. Acknowledgments

This work is supported by the National Key Research and Development Program of China under Grant No. 2021YFC3320103. In addition, we thank Kang Zhao for his help with this paper.

References

- [1] Tadas Baltrušaitis, Marwa Mahmoud, and Peter Robinson. Cross-dataset learning and person-specific normalisation for automatic action unit detection. In *2015 11th IEEE International Conference and Workshops on Automatic Face and Gesture Recognition (FG)*, volume 6, pages 1–6. IEEE, 2015. 7
- [2] Egor Burkov, Igor Pasechnik, Artur Grigorev, and Victor Lempitsky. Neural head reenactment with latent pose descriptors. In *Proceedings of the IEEE/CVF conference on computer vision and pattern recognition*, pages 13786–13795, 2020. 1, 3
- [3] Radek Daněček, Michael J Black, and Timo Bolkart. Emoca: Emotion driven monocular face capture and animation. In *Proceedings of the IEEE/CVF Conference on Computer Vision and Pattern Recognition*, pages 20311–20322, 2022. 1, 4, 7
- [4] Hui Ding, Kumar Sricharan, and Rama Chellappa. Exprgan: Facial expression editing with controllable expression intensity. In *Proceedings of the AAAI conference on artificial intelligence*, 2018. 1, 2
- [5] Michail Christos Doukas, Stefanos Zafeiriou, and Viktoriia Sharmanska. Headgan: One-shot neural head synthesis and editing. In *Proceedings of the IEEE/CVF International Conference on Computer Vision*, pages 14398–14407, 2021. 1, 3
- [6] Nikita Drobyshev, Jenya Chelishchev, Taras Khakhulin, Aleksei Ivakhnenko, Victor Lempitsky, and Egor Zakharov. Megaportraits: One-shot megapixel neural head avatars. *arXiv preprint arXiv:2207.07621*, 2022. 1, 3
- [7] Lijie Fan, Wenbing Huang, Chuang Gan, Junzhou Huang, and Boqing Gong. Controllable image-to-video translation: A case study on facial expression generation. In *Proceedings of the AAAI Conference on Artificial Intelligence*, pages 3510–3517, 2019. 2
- [8] Kuangxiao Gu, Yuqian Zhou, and Thomas Huang. Flnet: Landmark driven fetching and learning network for faithful talking facial animation synthesis. In *Proceedings of the AAAI conference on artificial intelligence*, pages 10861–10868, 2020. 3
- [9] Sungjoo Ha, Martin Kersner, Beomsu Kim, Seokjun Seo, and Dongyoung Kim. Marionette: Few-shot face reenactment preserving identity of unseen targets. In *Proceedings of the AAAI conference on artificial intelligence*, pages 10893–10900, 2020. 1, 3
- [10] Martin Heusel, Hubert Ramsauer, Thomas Unterthiner, Bernhard Nessler, and Sepp Hochreiter. Gans trained by a two time-scale update rule converge to a local nash equilibrium. *Advances in neural information processing systems*, 30, 2017. 7
- [11] Fa-Ting Hong, Longhao Zhang, Li Shen, and Dan Xu. Depth-aware generative adversarial network for talking head video generation. In *Proceedings of the IEEE/CVF Conference on Computer Vision and Pattern Recognition*, pages 3397–3406, 2022. 1, 3, 7
- [12] Gee-Sern Hsu, Chun-Hung Tsai, and Hung-Yi Wu. Dual-generator face reenactment. In *Proceedings of the IEEE/CVF Conference on Computer Vision and Pattern Recognition*, pages 642–650, 2022. 3
- [13] Yuge Huang, Yuhan Wang, Ying Tai, Xiaoming Liu, Pengcheng Shen, Shaoxin Li, Jilin Li, and Feiyue Huang. Curricularface: adaptive curriculum learning loss for deep face recognition. In *proceedings of the IEEE/CVF conference on computer vision and pattern recognition*, pages 5901–5910, 2020. 7
- [14] Amin Jourabloo, Fernando De la Torre, Jason Saragih, Shih-En Wei, Stephen Lombardi, Te-Li Wang, Danielle Belko, Autumn Trimble, and Hernan Badino. Robust egocentric photo-realistic facial expression transfer for virtual reality. In *Proceedings of the IEEE/CVF Conference on Computer Vision and Pattern Recognition*, pages 20323–20332, 2022. 3
- [15] Tero Karras, Timo Aila, Samuli Laine, and Jaakko Lehtinen. Progressive growing of gans for improved quality, stability, and variation. *arXiv preprint arXiv:1710.10196*, 2017. 7
- [16] Tero Karras, Samuli Laine, and Timo Aila. A style-based generator architecture for generative adversarial networks. In *Proceedings of the IEEE/CVF conference on computer vision and pattern recognition*, pages 4401–4410, 2019. 7
- [17] Tero Karras, Samuli Laine, Miika Aittala, Janne Hellsten, Jaakko Lehtinen, and Timo Aila. Analyzing and improving the image quality of stylegan. In *Proceedings of the IEEE/CVF conference on computer vision and pattern recognition*, pages 8110–8119, 2020. 4, 5
- [18] Oliver Langner, Ron Dotsch, Gijbert Bijlstra, Daniel HJ Wigboldus, Skyler T Hawk, and AD Van Knippenberg. Pre-

- sentation and validation of the radboud faces database. *Cognition and emotion*, 24(8):1377–1388, 2010. 7
- [19] Tianye Li, Timo Bolkart, Michael J Black, Hao Li, and Javier Romero. Learning a model of facial shape and expression from 4d scans. *ACM Trans. Graph.*, 36(6):194–1, 2017. 4
- [20] Jun Ling, Han Xue, Li Song, Shuhui Yang, Rong Xie, and Xiao Gu. Toward fine-grained facial expression manipulation. In *European Conference on Computer Vision*, pages 37–53. Springer, 2020. 1, 3, 7
- [21] Yueming Lyu, Tianwei Lin, Fu Li, Dongliang He, Jing Dong, and Tieniu Tan. Deltaedit: Exploring text-free training for text-driven image manipulation. In *Proceedings of the IEEE/CVF Conference on Computer Vision and Pattern Recognition*, pages 6894–6903, 2023. 3
- [22] Roey Mechrez, Itamar Talmi, and Lihi Zelnik-Manor. The contextual loss for image transformation with non-aligned data. In *Proceedings of the European conference on computer vision (ECCV)*, pages 768–783, 2018. 6
- [23] Ali Mollahosseini, Behzad Hasani, and Mohammad H Mahoor. Affectnet: A database for facial expression, valence, and arousal computing in the wild. *IEEE Transactions on Affective Computing*, 10(1):18–31, 2017. 7
- [24] Yuval Nirkin, Yosi Keller, and Tal Hassner. Fsgan: Subject agnostic face swapping and reenactment. In *Proceedings of the IEEE/CVF international conference on computer vision*, pages 7184–7193, 2019. 3
- [25] Xuesong Niu, Hu Han, Shiguang Shan, and Xilin Chen. Multi-label co-regularization for semi-supervised facial action unit recognition. *Advances in neural information processing systems*, 32, 2019. 6
- [26] Albert Pumarola, Antonio Agudo, Aleix M Martinez, Alberto Sanfeliu, and Francesc Moreno-Noguer. Ganimation: Anatomically-aware facial animation from a single image. In *Proceedings of the European conference on computer vision (ECCV)*, pages 818–833, 2018. 1, 2, 7
- [27] Xuebin Qin, Zichen Zhang, Chenyang Huang, Masood Dehghan, Osmar R Zaiane, and Martin Jagersand. U2-net: Going deeper with nested u-structure for salient object detection. *Pattern recognition*, 106:107404, 2020. 5
- [28] Yurui Ren, Ge Li, Yuanqi Chen, Thomas H Li, and Shan Liu. Pirenderer: Controllable portrait image generation via semantic neural rendering. In *Proceedings of the IEEE/CVF International Conference on Computer Vision*, pages 13759–13768, 2021. 7
- [29] Tim Salimans, Ian Goodfellow, Wojciech Zaremba, Vicki Cheung, Alec Radford, and Xi Chen. Improved techniques for training gans. *Advances in neural information processing systems*, 29, 2016. 8
- [30] Aliaksandr Siarohin, Stéphane Lathuilière, Sergey Tulyakov, Elisa Ricci, and Nicu Sebe. First order motion model for image animation. *Advances in Neural Information Processing Systems*, 32, 2019. 1, 3, 7
- [31] Lingxiao Song, Zhihe Lu, Ran He, Zhenan Sun, and Tieniu Tan. Geometry guided adversarial facial expression synthesis. In *Proceedings of the 26th ACM international conference on Multimedia*, pages 627–635, 2018. 1, 2
- [32] Hao Tang, Wei Wang, Songsong Wu, Xinya Chen, Dan Xu, Nicu Sebe, and Yan Yan. Expression conditional gan for facial expression-to-expression translation. In *2019 IEEE International Conference on Image Processing (ICIP)*, pages 4449–4453. IEEE, 2019. 1, 3
- [33] Justus Thies, Michael Zollhöfer, Matthias Nießner, Levi Valgaerts, Marc Stamminger, and Christian Theobalt. Real-time expression transfer for facial reenactment. *ACM Trans. Graph.*, 34(6):183–1, 2015. 2
- [34] Justus Thies, Michael Zollhofer, Marc Stamminger, Christian Theobalt, and Matthias Nießner. Face2face: Real-time face capture and reenactment of rgb videos. In *Proceedings of the IEEE conference on computer vision and pattern recognition*, pages 2387–2395, 2016. 2
- [35] Soumya Tripathy, Juho Kannala, and Esa Rahtu. Icfac: Interpretable and controllable face reenactment using gans. In *Proceedings of the IEEE/CVF winter conference on applications of computer vision*, pages 3385–3394, 2020. 3
- [36] Ashish Vaswani, Noam Shazeer, Niki Parmar, Jakob Uszkoreit, Llion Jones, Aidan N Gomez, Łukasz Kaiser, and Illia Polosukhin. Attention is all you need. *Advances in neural information processing systems*, 30, 2017. 4
- [37] Jinghui Wang, Jie Zhang, Zijia Lu, and Shiguang Shan. Dfnet: Disentanglement of face deformation and texture synthesis for expression editing. In *2019 IEEE International Conference on Image Processing (ICIP)*, pages 3881–3885. IEEE, 2019. 3
- [38] Ting-Chun Wang, Arun Mallya, and Ming-Yu Liu. One-shot free-view neural talking-head synthesis for video conferencing. In *Proceedings of the IEEE/CVF conference on computer vision and pattern recognition*, pages 10039–10049, 2021. 1, 3, 7
- [39] Xueping Wang, Weixin Li, Guodong Mu, Di Huang, and Yunhong Wang. Facial expression synthesis by u-net conditional generative adversarial networks. In *Proceedings of the 2018 ACM on International Conference on Multimedia Retrieval*, pages 283–290, 2018. 1, 2
- [40] Rongliang Wu, Gongjie Zhang, Shijian Lu, and Tao Chen. Cascade ef-gan: Progressive facial expression editing with local focuses. In *Proceedings of the IEEE/CVF Conference on Computer Vision and Pattern Recognition*, pages 5021–5030, 2020. 3
- [41] Chao Yang and Ser-Nam Lim. Unconstrained facial expression transfer using style-based generator. *arXiv preprint arXiv:1912.06253*, 2019. 2
- [42] Kewei Yang, Kang Chen, Daoliang Guo, Song-Hai Zhang, Yuan-Chen Guo, and Weidong Zhang. Face2facerho: Real-time high-resolution one-shot face reenactment. In *European Conference on Computer Vision*, pages 55–71. Springer, 2022. 2, 3, 5, 7
- [43] Songlin Yang, Wei Wang, Bo Peng, and Jing Dong. Designing a 3d-aware stylenerf encoder for face editing. In *ICASSP 2023-2023 IEEE International Conference on Acoustics, Speech and Signal Processing (ICASSP)*, pages 1–5. IEEE, 2023. 3
- [44] Raymond Yeh, Ziwei Liu, Dan B Goldman, and Aseem Agarwala. Semantic facial expression editing using autoencoded flow. *arXiv preprint arXiv:1611.09961*, 2016. 1, 2

- [45] Fei Yin, Yong Zhang, Xiaodong Cun, Mingdeng Cao, Yanbo Fan, Xuan Wang, Qingyan Bai, Baoyuan Wu, Jue Wang, and Yujiu Yang. Styleheat: One-shot high-resolution editable talking face generation via pretrained stylegan. *arXiv preprint arXiv:2203.04036*, 2022. [3](#), [7](#)
- [46] Jiangning Zhang, Xianfang Zeng, Mengmeng Wang, Yusu Pan, Liang Liu, Yong Liu, Yu Ding, and Changjie Fan. Freenet: Multi-identity face reenactment. In *Proceedings of the IEEE/CVF conference on computer vision and pattern recognition*, pages 5326–5335, 2020. [3](#)
- [47] Richard Zhang, Phillip Isola, Alexei A Efros, Eli Shechtman, and Oliver Wang. The unreasonable effectiveness of deep features as a perceptual metric. In *Proceedings of the IEEE conference on computer vision and pattern recognition*, pages 586–595, 2018. [5](#)